PAPER *Special Issue on Techniques for Constructing Microwave Simulators*

Microwave Simulator Based on the Finite-Element Method by Use of Commercial Tools

Koichi HIRAYAMA[†a)], **Yoshio HAYASHI**[†], *and* **Masanori KOSHIBA**[††], ***Regular Members***

SUMMARY Making up a microwave simulator is tried, which has an analysis method based on the finite-element method as a solver and commercial tools as a pre- and post-processor of a graphical user interface. The platform of this simulator is Windows, but, since the codes and configuration files to be created are common on Windows, Unix, and Linux, the simulator running on any platform may be made up at the same time, except a document on which all the commands of the simulator are embedded and executable. Using the simulator, the transmission properties of a 2- and 3-D waveguide discontinuity in a microwave circuit and eigenmodes of a 2- and 3-D waveguide are analyzed, and the computed results are presented in graphs of S parameters and plots of the electric field distribution.

key words: *microwave simulator, FEM, 3-D analysis, waveguide discontinuity, eigenmode*

1. Introduction

A number of researchers engaged in numerical analysis have intensively developed solvers based on their novel formulations, but most of them, especially in universities, have not paid much attention in making up a simulator with a pre- and post-processor for their solvers. When the researchers use the solvers developed by themselves, they may not feel to need the pre- and post-processor, because they may give to the solvers various data necessary for the analysis in text style with no sense of difficulty, and can alter the source code of the solvers freely for the convenience of the computation. On the other hand, though some solvers may be applicable to various types of microwave circuits with complicated geometry, the researchers may not able to make the best use of them since it is difficult or impossible to give geometry data in text style, including geometry of a microwave circuit, boundary conditions, and division of a domain if necessary. Also, the visualization of numerical results in a post-processor, for example, graphs of S parameters and plots of electromagnetic field distributions, plays an important role in the knowledge of the physical meaning of the results and the design of the circuit.

In order to make up a simulator with a pre- and post-processor of a graphical user interface (GUI), one is required to have knowledge of the programming on a particular window system of a platform (Windows [1], Unix, Linux, etc.). Also, a mesh generator, a software tool which divides a surface or volume into a number of small subdomains automatically, should be added to a pre-processor for some solvers, especially those based on the finite-element method (FEM). Therefore we guess it is a difficult task for researchers to make a pre- and post-processor of a GUI.

In this paper, we try making up a microwave simulator in an easy way. This simulator has an analysis method based on the FEM as a solver and commercial tools as a pre- and post-processor of a GUI. The platform of the simulator is Windows, and the pre- and post-processor are GiD [2] and MATLAB [3], respectively. To make up the simulator, one must create the source codes of a solver, some configuration files for the data format in GiD, and some codes for the visualization of graphs and plots in MATLAB, but, fortunately, since their codes and files are common on Windows, Unix, and Linux, one can make up the simulator running on any platform at the same time. Using this simulator, the transmission properties of a 2- and 3-D waveguide discontinuity in a microwave circuit and eigenmodes of a 2- and 3-D waveguide are analyzed, and the computed results are presented in graphs of S parameters and plots of the electric field distribution.

2. Solvers

2.1 H-Plane Waveguide Discontinuity

We consider an H-plane waveguide discontinuity, as shown in Fig. 1, where boundary Γ_0 is a perfect conductor, and boundary Γ_i $(i = 1, 2, \cdots, N)$ connects the discontinuity region Ω to the uniform waveguide i of width d_i. Assuming that there is no variation of fields and refractive indices in the z direction, we can obtain the following functional with respect to $\phi = E_z$ (E_z being the z component of the electric field):

$$F(\phi) = \frac{1}{2}\iint_{\Omega}[(\nabla\phi)^2 - k_0^2\varepsilon_r\phi^2]dxdy + \frac{1}{2}\sum_{i=1}^{N}\int_0^{d_i}\phi_i P_i(\phi_i)dy_i - \int_0^{d_1}\phi_1 Q dy_1 \quad (1)$$

Manuscript received December 11, 2000.

[†]The authors are with the Department of Electrical and Electronic Engineering, Kitami Institute of Technology, Kitami-shi, 090-8507 Japan.

[††]The author is with the Division of Electronics and Information Engineering, Hokkaido University, Sapporo-shi, 060-8628 Japan.

a) E-mail: hira@elec.kitami-it.ac.jp

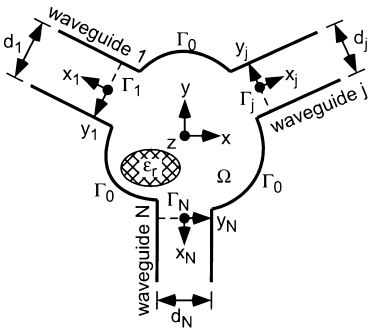

Fig. 1 H-plane waveguide discontinuity.

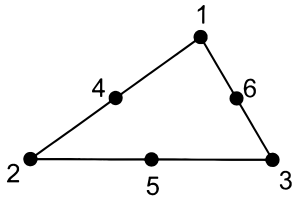

Fig. 2 Quadratic triangular element.

where k_0 is a wavenumber in vacuum, ε_r represents a relative permittivity of material, and ϕ_i denotes ϕ on Γ_i. The symbol $P_i(\phi_i)$ is expressed with the propagation constants and the mode-function of the eigenmodes in waveguide i, and Q denotes an incident wave from waveguide 1.

Applying the variational principle to Eq. (1), dividing and discretizing region Ω by quadratic triangular elements shown in Fig. 2, we obtain the following matrix equation:

$$[A]\{\phi\} + \sum_{i=1}^{N}[P_i]\{\phi_i\} = \{Q\} \tag{2}$$

where the components of vector $\{\phi\}$ are the values of ϕ at the nodes of the elements in Ω except on perfect conductor, and the components of vector $\{\phi_i\}$ are the values at the nodes on Γ_i. Since the right-hand side of Eq. (2) has a sparse and complex matrix, the final matrix equation can be solved efficiently with much reduction of computational time and memory through the bi-conjugate gradient method [6] after computing the incomplete LU decomposition of the matrix.

2.2 Shielded Planar Transmission Line

We consider a shielded planar transmission line having uniform cross section Ω along the z axis, as shown in Fig. 3, where boundary Γ_0 is a perfect conductor. We can obtain the following functional with respect to the electric field $\boldsymbol{E}$:

$$F(\boldsymbol{E}) = \iint_{\Omega}[(\nabla \times \boldsymbol{E})^* \cdot (\nabla \times \boldsymbol{E}) - k_0^2 \varepsilon_r \boldsymbol{E}^* \cdot \boldsymbol{E}]dxdy \tag{3}$$

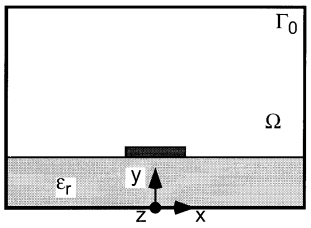

Fig. 3 Shielded planar transmission line.

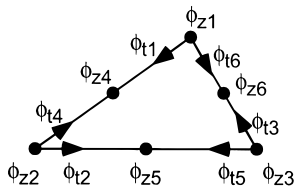

Fig. 4 Triangular edge/nodal element.

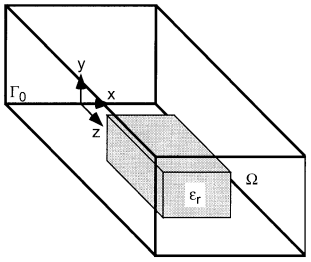

Fig. 5 3-D cavity resonator.

where the superscript $*$ denotes the complex conjugate.

Applying the variational principle to Eq. (3), dividing and discretizing region Ω by triangular edge/nodal elements based on linear tangential and linear normal vector basis functions, as shown in Fig. 4 [4], we obtain the following matrix equation:

$$[A]\{\phi\} = \beta^2[B]\{\phi\} \tag{4}$$

where β is a propagation constant in the z direction, the components of vector $\{\phi\}$ are the values of the electric field at the sides and nodes of the elements in Ω except those tangential to perfect conductor. Because both $[A]$ and $[B]$ are sparse matrices, the generalized eigenvalue problem of Eq. (4) can be solved efficiently with much reduction of computational time and memory through the subspace method [7] if an appropriate initial value for β is given.

2.3 3-D Cavity Resonator

We consider a 3-D cavity resonator enclosed by a perfect conductor Γ_0, as shown in Fig. 5, where Ω denotes the internal region of the cavity resonator. We can obtain the following functional with respect to the electric field $\boldsymbol{E}$:

$$F(\boldsymbol{E}) = \iiint_{\Omega}[(\nabla \times \boldsymbol{E}) \cdot (\nabla \times \boldsymbol{E})$$

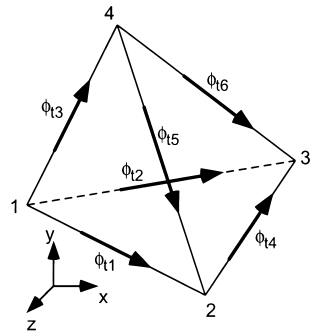

Fig. 6 Tetrahedral edge element.

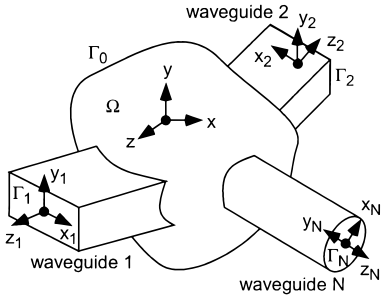

Fig. 7 3-D waveguide discontinuity in a microwave circuit.

$$- k_0^2 \varepsilon_r \boldsymbol{E} \cdot \boldsymbol{E}] dxdydz \tag{5}$$

Applying the variational principle to Eq. (5), dividing and discretizing region Ω by tetrahedral edge elements shown in Fig. 6 [5], we obtain the following matrix equation:

$$[A]\{\phi\} = k_0^2 [B]\{\phi\} \tag{6}$$

where the components of vector $\{\phi\}$ are the values of the electric field at the sides of the elements in Ω except those tangential to perfect conductor. Because $[A]$ is a sparse matrix and $[B]$ is a sparse and positive-definitive matrix, the generalized eigenvalue problem of Eq. (6) can be solved efficiently with much reduction of computational time and memory through the subspace method [7] if an appropriate initial value for k_0 is given.

2.4 3-D Waveguide Discontinuity

We consider a 3-D waveguide discontinuity in a microwave circuit, as shown in Fig. 7, where boundary Γ_0 is a perfect conductor, and boundary Γ_i ($i = 1, 2, \cdots, N$) connects the discontinuity region Ω to the uniform waveguide i. We can obtain the following functional with respect to the electric field $\boldsymbol{E}$:

$$\begin{aligned} F(\boldsymbol{E}) = & \frac{1}{2} \iiint_{\Omega} [(\nabla \times \boldsymbol{E}) \cdot (\nabla \times \boldsymbol{E}) \\ & - k_0^2 \varepsilon_r \boldsymbol{E} \cdot \boldsymbol{E}] \, dxdydz \\ & + \frac{1}{2} \sum_{i=1}^{N} \iint_{\Gamma_i} \boldsymbol{E}_i \cdot \boldsymbol{P}_i(\boldsymbol{E}_i) dx_i dy_i \\ & - \iint_{\Gamma_1} \boldsymbol{E}_1 \cdot \boldsymbol{Q} dx_1 dy_1 \end{aligned} \tag{7}$$

where $\boldsymbol{E}_i$ denotes $\boldsymbol{E}$ on Γ_i. Here the uniform waveguides are formulated based on the eigenmode expansion, and the eigenmodes are calculated numerically using the FEM, because eigenmodes of uniform waveguides may not be expressed analytically. The symbol $\boldsymbol{P}_i(\boldsymbol{E}_i)$ is expressed with the propagation constants and the mode-function of the eigenmodes in waveguide i, and $\boldsymbol{Q}$ denotes an incident wave from waveguide 1.

Applying the variational principle to Eq. (7), dividing and discretizing region Ω by tetrahedral edge elements shown in Fig. 6, we obtain the following matrix equation:

$$[A]\{\phi\} + \sum_{i=1}^{N} [P_i]\{\phi_i\} = \{Q\} \tag{8}$$

where the components of vector $\{\phi\}$ are the values of the electric field at the sides of the elements in Ω except on perfect conductor, and the components of vector $\{\phi_i\}$ are the values at the sides on Γ_i. Since the right-hand side of Eq. (8) has a sparse and complex matrix, the final matrix equation can be solved efficiently with much reduction of computational time and memory through the bi-conjugate gradient method [6] after computing the incomplete LU decomposition of the matrix.

3. Pre-Processor

There are a number of commercial or public-domain tools which can define various types of geometry of microwave circuits and then divide a surface into triangular elements in a 2-D waveguide or a volume into tetrahedral elements in a 3-D waveguide. These tools are surveyed in the following homepages:

1. http://www.andrew.cmu.edu/user/sowen /mesh.html
2. http://www-users.informatik.rwth-aachen.de /~roberts/meshgeneration.html
3. http://www.engr.usask.ca/~macphed /finite/fe_resources/fe_resources.html

Some of the tools listed in the first homepage are shown in Table 1, which are available via the internet and usable free of charge (in a limited period or function). We decided to use GiD [2], because GiD can define geometry through a GUI. GiD is a commercial tool, but is usable free of charge within a month or in the limitation of less than 700 triangular elements and 3000 tetrahedral elements.

4. Post-Processor

We adopt MATLAB [3] as a post-processor which can draw graphs of S parameters and plots of electric field

Table 1 Examples of mesh generators.

product name	comment
COG	library in C++
Geompack90	no subdivision of given lines
GiD	graphical user interface (GUI)
GRUMMP	character-based user interface (CUI)
Qhull	subdivision of only convex domain
QMG	character-based user interface (CUI)

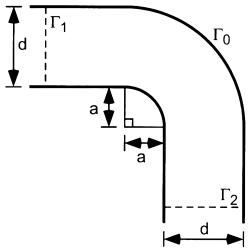

Fig. 8 Right-angle circular bend in an H-plane of a hollow wavegude.

in contours or arrows. MATLAB is a commercial, widely-used tool having a programming language for numerical computation and visualization. Moreover, since one can create a document of Word [1], called M-book, which contains executable MATLAB codes annotated with text, we can easily make up a simulator on an M-book, where all the commands in our simulator, including the execution of GiD, solvers, and text editors as well as MATLAB codes, are embedded. Also, it is convenient for users of the simulator that the output of the MATLAB codes, that is, graphs and plots for numerical results, is saved on the document of Word.

5. Numerical Computation by Use of Simulator

5.1 Right-Angle Circular Bend in H-Plane

We analyze the transmission characteristics of a right-angle circular bend in an H-plane of a hollow waveguide, as shown in Fig. 8 [8], where the TE_{10} mode incidence is assumed.

Figure 9 shows a screen of a pre-processor of our simulator at $C = 0.1$, where $C = a/(a + d)$. First we execute a command embedded on a document to run GiD. After creating arcs and line segments to define the geometry, and assigning to them the indices of the boundary condition, whose value corresponds to the subscript of boundary Γ_i, we divide a surface surrounded by boundaries Γ_0 to Γ_2 into triangular elements by using a mesh generator involved in GiD. The resulting data is written into a file named preout.dat, and the element division is shown on a document of Word by using a MATLAB code named drawtri.

Figure 10 shows a screen of a solver of our simulator. We must create a file named femin.dat to specify various calculational parameters. Figure 11 shows

1. Pre–processor
1. 1 Definition of geometry
!\win32app\GiDWin60\gid.exe
1.2 Display of element division
・required data file: preout.dat
drawtri

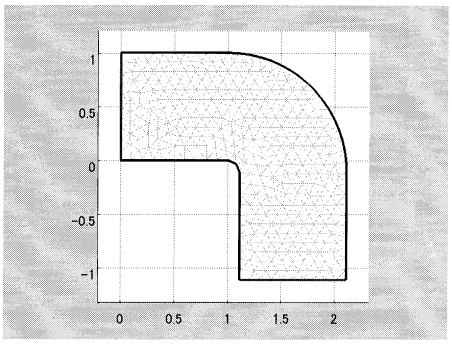

Fig. 9 Screen of pre-processor.

2. Solver
2.1 Calculational parameters
!notepad femin.dat
・required data file: preout.dat, femin.dat
2.2 H–plane waveguide discontinuity
・Quadratic triangular element
!hollow\i386\hollow.exe
2.3 Eigenmode of shielded planar transmission line
・Triangular edge/nodal element
!mwlinesp\i386\edgesp.exe
2.4 Eigenmode of 3–D cavity resonator
・Tetrahedral edge element
!reso3dsp\i386\edgesp.exe
2.5 3–D waveguide discontinuity in microwave circuit
・Tetrahedral edge element
!hollow3d\i386\edge.exe

Fig. 10 Screen of solver.

```
11 1 19 3.141592653589793d-1
6
1
1 1 1 1.0
11 100 100
```

Fig. 11 Calculational parameters in femin.dat.

an example of femin.dat. The first row gives an initial, incremental, and terminal values and a factor of $k_0 d_0$ (d_0 being the length assumed as unity in defining geometry in GiD), and this example represents $k_0 d_0 = 11 \times (\pi/10), 12 \times (\pi/10), \cdots, 19 \times (\pi/10)$. The second row specifies the number of eigenmodes taken into account in the eigenmode expansion of the uniform waveguides. The third row specifies the number of material, and the fourth row gives an initial, incremental, and terminal values and a factor of the relative permittivity of the material defined as index 1 in GiD. The fifth row specifies at $k_0 d_0 = 11 \times (\pi/10)$ to compute the electric field distribution at the points where the lines dividing the width of the x and y directions into 100 subsections intersect each other. After saving femin.dat and executing our solver named hollow.exe for the anal-

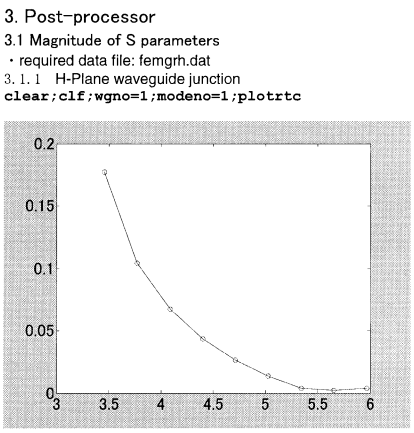

Fig. 12 Screen of post-processor.

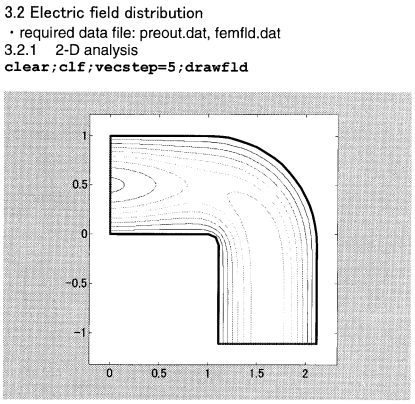

Fig. 13 Another screen of post-processor.

ysis of an H-plane waveguide discontinuity, femlog.txt for full computational results, femfld.dat for the plots of the electric field distribution, and femgrh.dat for the graphs of S parameters will be created.

Figure 12 shows a screen of a post-processor of our simulator, where the magnitude of an S parameter is drawn in a graph by executing a MATLAB code named plotrtc. In this figure, the horizontal axis is $k_0 d_0$ given in femin.dat, and the vertical one is the magnitude of S_{11}, because the parameters of wgno=1 and modeno=1 mean the first mode of waveguide 1. If setting wgno=2, one will see the graph of the magnitude of S_{21}. Also, Fig. 13 shows another screen of a post-processor, where the magnitudes of the electric field are drawn in contours by executing a MATLAB code named drawfld. In this computation, the number of the triangular elements was 637, the number of the unknowns in the final Eq. (2) was 1234, and the required memory was about 1.7 MB.

Using our simulator six times, we obtained the results for various values of parameter C, and the magnitude of the reflected coefficient is shown in Fig. 14. Our results agree well with those of the normal mode analysis [8].

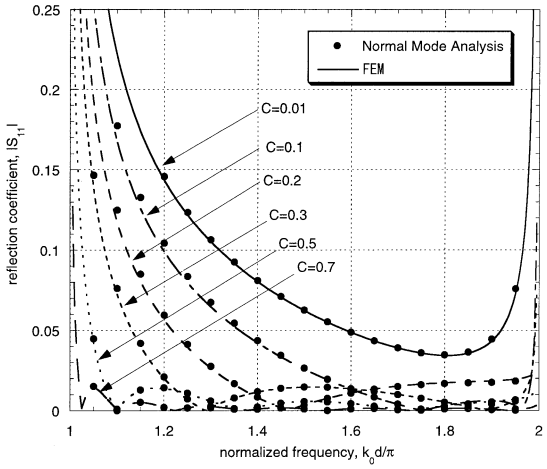

Fig. 14 S parameter of right-angle circular bend in H-plane.

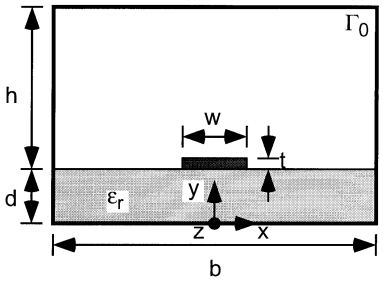

Fig. 15 Shielded microstrip line.

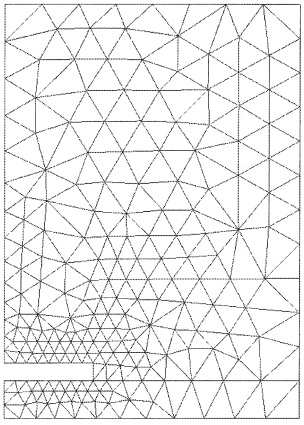

Fig. 16 Element division of shielded microstrip line.

5.2 Eigenmode of Shielded Microstrip Line

We compute the eigenmode of a shielded microstrip line, as shown in Fig. 15, where the width and thickness of the strip made of perfect conductor are respectively $w = 3\,\text{mm}$ and $t = 0.3\,\text{mm}$, the thickness and the relative permittivity of the substrate are respectively $d = 0.635\,\text{mm}$ and $\varepsilon_r = 9.8$ [9], and the size of the shielding conductor is $b = 10\,\text{mm}$ and $h = 6.35\,\text{mm}$ [10]. Figure 16 shows a screen of the element division

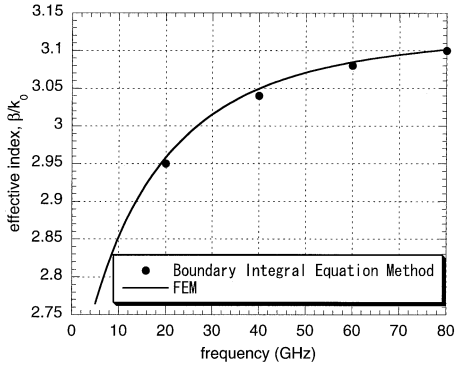

Fig. 17 Effective index of shielded microstrip line.

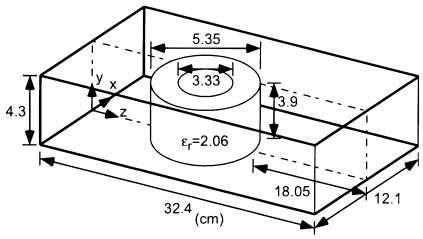

Fig. 18 3-D cavity resonator in which a teflon ring is partially loaded.

in GiD. For the symmetry of the waveguide, only a half region of $x \geq 0$ was divided and analyzed. A typical size of a triangular edge/nodal element was specified as 0.2 mm at the sides of the strip and 0.6 mm elsewhere. In this computation, the number of the triangular elements was 390, the number of the unknowns in the final Eq. (4) was 1885, and the required memory was about 3.6 MB. Figure 17 shows the effective index β/k_0 versus frequency. Our results agree well with those for the microstrip line without the shielding conductor by the boundary integral equation method [9].

5.3 Eigenmode of 3-D Cavity Resonator

We compute the eigenmode of a rectangular-parallelepiped cavity resonator in which a teflon ring is partially loaded, as shown in Fig. 18. Figure 19 shows a screen of the element division in GiD. For the symmetry of the resonator, only a half region of $x \geq 0$ was divided and analyzed. A typical size of a tetrahedral edge element was specified as 1 cm everywhere. In this computation, the number of the tetrahedral elements was 4757, the number of the unknowns in the final Eq. (6) was 4826, and the required memory was about 7.8 MB. The calculated resonant frequency of the lowest mode was 1.2563 GHz, close to 1.2571 GHz of the measured value [11].

5.4 Dielectric-Loaded Waveguide

We analyze the transmission characteristics of a

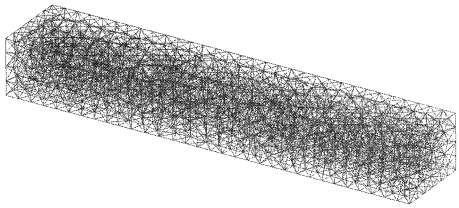

Fig. 19 Element division of the 3-D cavity resonator.

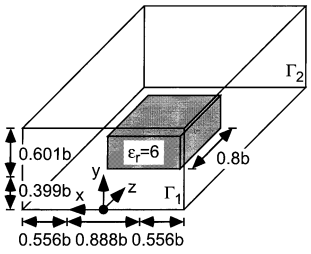

Fig. 20 Dielectric-loaded waveguide.

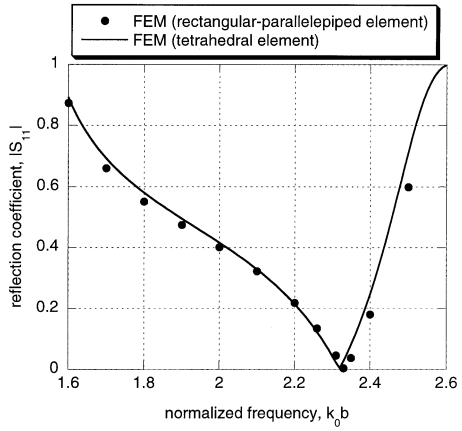

Fig. 21 S parameter of the dielectric-loaded waveguide.

dielectric-loaded waveguide, as shown in Fig. 20, where the TE_{10} mode incidence is assumed. For the symmetry of the waveguide, only a half region of $x \geq 0$ was divided and analyzed. A typical size of a tetrahedral edge element was specified as $0.25b$ everywhere. In this computation, the number of the tetrahedral elements was 800, the number of the unknowns in the final Eq. (8) was 859, and the required memory was about 1.3 MB. Figure 21 shows the S parameter versus normalized frequency, where a propagating mode and five evanescent modes are taken into account on each of boundaries Γ_1 and Γ_2. Our results agree well with those of the FEM with the rectangular-parallelepiped edge element [12]. Since the waveguide cross section on boundaries Γ_1 and Γ_2 is a hollow rectangular waveguide, the eigenmodes can be obtained analytically and were used in the formulation of Ref. [12]. But, to show the validity of our approach, we computed them here by the FEM with the triangular edge/nodal element based on constant tangential and linear normal vector basis functions [4].

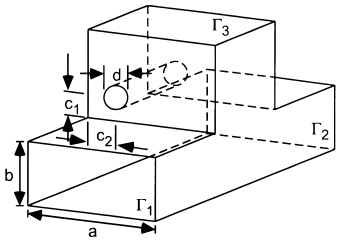

Fig. 22 T-branch circuit.

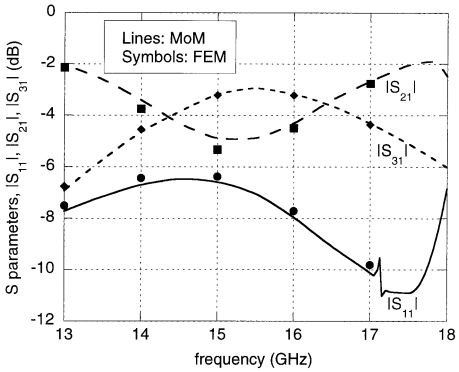

Fig. 23 S parameters of the T-branch circuit.

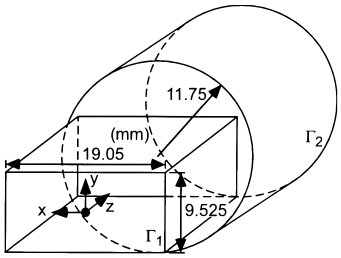

Fig. 24 Junction between rectangular and circular waveguides.

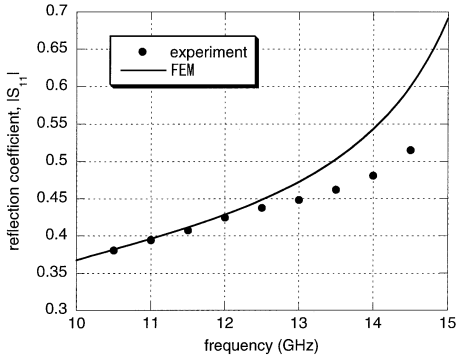

Fig. 25 S parameter of the junction between rectangular and circular waveguides.

5.5 T-Branch Circuit

We analyze the transmission characteristics of a T-branch circuit with a conductor post of diameter d, as shown in Fig. 22, where $a = 15.7988\,\text{mm}$, $b = 7.8994\,\text{mm}$, $c_1 = 2.5\,\text{mm}$, $c_2 = 4\,\text{mm}$, $d = 3\,\text{mm}$, and the TE_{10} mode incidence is assumed. A typical size of a tetrahedral edge element was specified as 1 mm everywhere. In this computation, the number of the tetrahedral elements was 15354, the number of the unknowns in the final Eq. (8) was 16528, and the required memory was about 43.9 MB. Figure 23 shows the S parameters versus frequency, where a propagating mode and five evanescent modes are taken into account on each of boundaries Γ_1 to Γ_3. Our results agree well with those of the method of moments [13]. Since the waveguide cross section on boundaries Γ_1 to Γ_3 is a hollow rectangular waveguide, the eigenmodes can be obtained analytically and were used in the formulation of Ref. [13]. But, to show the validity of our approach, we computed them here by the FEM with the triangular edge/nodal element.

5.6 Junction between Rectangular and Circular Waveguides

We analyze the transmission characteristics of a junction between rectangular and circular waveguides, as shown in Fig. 24, where the TE_{10} mode incidence is assumed. For the symmetry of the waveguide, only a quarter region of $x \geq 0$ and $y \geq 0$ was divided and analyzed. A typical size of a tetrahedral edge element was specified as 1 mm everywhere. In this computation, the number of the tetrahedral elements was 4073, the number of the unknowns in the final Eq. (8) was 4579, and the required memory was about 15.8 MB. Figure 25 shows the S parameter versus frequency, where a propagating mode and five evanescent modes are taken into account on each of boundaries Γ_1 and Γ_2. Our results agree with those of the measured values [13] for low frequency, but not for high frequency.

6. Conclusion

We tried to make up a microwave simulator in an easy way, whose simulator has an analysis method based on the FEM as a solver and commercial tools as a pre- and post-processor of a GUI. The platform of the simulator is Windows, but, since the codes and configuration files to be created are common on Windows, Unix, and Linux, we can make up the simulator running on any platform at the same time, except a document on which all the commands of the simulator are embedded and executable. Using the simulator, the transmission properties and eigenmodes of a 2-D and 3-D waveguides were analyzed, and the computed results were presented in graphs of S parameters and plots of the electric field distribution.

In the future, we will add the analysis method for a microwave circuit of an open structure, using the perfectly matched layer [15].

References

[1] http://www.microsoft.com/
[2] http://gid.cimne.upc.es/
[3] http://www.mathworks.com/products/matlab/
[4] M. Koshiba and Y. Tsuji, "Curvilinear hybrid edge/nodal elements with triangular shape for guided-wave problems," J. Lightwave Technol., vol.18, no.5, pp.737–743, May 2000.
[5] J. Jin, The Finite Element Method in Electromagnetics, John Wiley & Sons, New York, 1993.
[6] R. Barrett, M. Berry, T.F. Chan, J. Demmel, J. Donato, J. Dongarra, V. Eijkhout, R. Pozo, C. Romine, and H. Van der Vorst, Templates for the Solution of Linear Systems: Building Blocks for Iterative Methods, SIAM, Philadelphia, 1994.
[7] F.A. Fernandez, J.B. Davies, S. Zhu, and Y. Lu, "Sparse matrix eigenvalue solver for finite element solution of dielectric waveguides," Electron. Lett., vol.27, no.20, pp.1824–1826, Sept. 1991.
[8] J.-P. Hsu and T. Anada, "Systematic analysis method of E- and H-plane circular bend of rectangular waveguide based on the planar circuit equations and equivalent network representation," IEEE MTT-S Int. Microwave Symp. Dig., vol.2, pp.749–752, May 1995.
[9] F. Olyslager, D.D. Zutter, and K. Blomme, "Rigorous analysis of the propagation characteristics of general lossless and lossy multiconductor transmission lines in multilayered media," IEEE Trans. Microwave Theory & Tech., vol.41, no.1, pp.79–88, Jan. 1993.
[10] M.S. Alam, K. Hirayama, Y. Hayashi, and M. Koshiba, "Analysis of shielded microstrip lines with arbitrary metallization cross section using a vector finite element method," IEEE Trans. Microwave Theory & Tech., vol.42, no.11, pp.2112–2117, Nov. 1994.
[11] I. Bardi, O. Biro, K. Preis, G. Vrisk, and K.R. Richter, "Nodal and edge element analysis of inhomogeneously loaded 3D cavities," IEEE Magn., vol.28, no.2, pp.1142–1145, March 1992.
[12] K. Ise, K. Inoue, and M. Koshiba, "Three-dimensional finite-element method with edge elements for electromagnetic waveguide discontinuities," IEEE Trans. Microwave Theory & Tech., vol.39, no.8, pp.1289–1295, Aug. 1991.
[13] R. Bunger and F. Arndt, "Moment-method analysis of arbitrary 3-D metallic N-port waveguide structures," IEEE Trans. Microwave Theory & Tech., vol.48, no.4, pp.531–537, April 2000.
[14] R. Keller and F. Arndt, "Rigorous modal analysis of the asymmetric rectangular iris in circular waveguide," IEEE Microwave & Guided Wave Lett., vol.3, no.6, pp.185–187, June 1993.
[15] J.P. Berenger, "A perfectly matched layer for the absorption of electromagnetic waves," J. Comput. Phys., vol.114, no.2, pp.110–117, Oct. 1994.

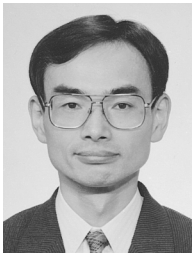

Koichi Hirayama was born in Shiranuka, Hokkaido, Japan, on September 8, 1961. He received the B.S., M.S., and Ph.D. degrees in electronic engineering from Hokkaido University, Sapporo, Japan, in 1984, 1986, and 1989, respectively. In 1989, he joined the Department of Electronic Engineering, Kushiro National College of Technology, Kushiro, Japan. In 1992, he became an Associate Professor of Electronic Engineering at Kitami Institute of Technology, Kitami, Japan. He has been interested in the analysis of propagation and scattering characteristics in electromagnetic and optical waveguides. Dr. Hirayama is a member of the Japan Society of Applied Physics and a senior member of the Institute of Electrical and Electronic Engineers (IEEE).

Yoshio Hayashi was born in Tokyo, Japan, on October 28, 1937. He received the B.E. degree in electrical engineering from Chiba University, Chiba, Japan, in 1961, and the M.E. and Ph.D. degrees in electronics engineering from Hokkaido University, Sapporo, Japan, in 1965 and 1972, respectively. He served in the Japan Self-Defense Air Force from 1961 to 1969. He was a Visiting Scholar of Electrical Engineering at the University of Illinois, Urbana, from 1981 to 1982. Currently, he is a Professor of Electrical and Electronic Engineering at Kitami Institute of Technology, Kitami, Japan. He has been engaged in research on microwave field theory and electromagnetic wave problems. Dr. Hayashi is a member of the Image Information and Television Engineers of Japan.

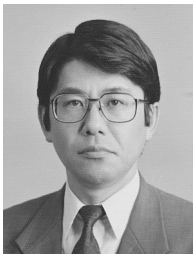

Masanori Koshiba was born in Sapporo, Japan, on November 23, 1948. He received the B.S., M.S., and Ph.D. degrees in electronic engineering from Hokkaido University, Sapporo, Japan, in 1971, 1973, and 1976, respectively. In 1976, he joined the Department of Electronic Engineering, Kitami Institute of Technology, Kitami, Japan. From 1979 to 1987, he was an Associate Professor of Electronic Engineering at Hokkaido University, and in 1987, he became a Professor. He has been engaged in research on wave electronics, including microwaves, millimeter-waves, lightwaves, surface acoustic waves (SAW), magnetostatic waves (MSW), and electron waves, and computer-aided design and modeling of guided-wave devices using finite element method, boundary element method, beam propagation method, etc. He is an author or coauthor of more than 200 research papers in English and of more than 100 research papers in Japanese both in refereed journals. He authored the books *Optical Waveguide Analysis* (New York: McGraw-Hill) and *Optical Waveguide Theory by the Finite Element Method* (Tokyo/Dordrecht: KTK Scientific/Kluwer), and coauthored the books *Analysis Methods for Electromagnetic Wave Problems* (Norwood, MA: Artech House), *Ultrafast and Ultra-parallel Optoelectronics* (New York: Wiley), and *Finite Element Software for Microwave Engineering* (New York: Wiley). Dr. Koshiba is a member of the Institute of Electrical Engineers of Japan, the Institute of Image Information and Television Engineers of Japan, the Japan Society for Simulation Technology, the Japan Society for Computational Methods in Engineering, Japan Society of Applied Electromagnetics and Mechanics, the Japan Society for Computational Engineering and Science, and the Applied Computational Electromagnetics Society (ACES), and a senior member of the Institute of Electrical and Electronic Engineers (IEEE). In 1987, 1997, and 1999, he received the Excellent Paper Awards from the IEICE, and in 1998, he received the Electronics-Society Award from the IEICE.